

# **Multiple Slip Conditions on MHD Carreau Dusty Fluidover Sheet with Cattaneo-Christov Heat Flux and Thermal Radiation**

Mamatha Sadandha Upadhyay<sup>1</sup>, Mahesha<sup>2</sup>, Chakravarthula Siva Krishnam Raju<sup>3</sup>, Shaik Mohammed  
Ibrahim<sup>4</sup>, Giulio Lorenzini<sup>5\*</sup>

<sup>1</sup>Department of Mathematics, Garden City College of Science and Management Studies, Karnataka, India<sup>1</sup>

<sup>2</sup>Department of Mathematics, University BDT College of Engineering, Karnataka, India

<sup>3</sup>Department of Mathematics, VIT University, Vellore, India

<sup>4</sup>Department of Mathematics, GITAM University, Andhra Pradesh, India

<sup>5</sup>Department of Engineering and Architecture, University of Parma, Italy

**Abstract:** Essence of the present study is to investigate the combined impact of thermal conductivity and non-Fourier heat flux model of the steady boundary layer flow of a Carreau Dusty Fluid past a stretching sheet in the presence of slip conditions. Similarity transformations are considered to transform the governing non-linear partial differential equations into nonlinear ordinary differential equations. The transformed ODEs are solved numerically by employing Runge-Kutta Fehlberg Scheme (RKFS). To interpret the influence of flow parameters on the fluid velocity, temperature and concentration profiles graphs and tables were developed and the results are discussed. The present results are validated by comparing with the published results and noticed favorable agreement. Our result implies that the rate of heat transfer significantly increases with the enhancement of thermal radiation parameters and an opposite influence is observed due to the thermal relaxation time in case of both fluid and dust phase. When we incorporate dust particles in the flow, dust particle opposes the flow, hence the momentum, thermal and concentration profiles are decreasing in dust phase. Thus we conclude that dust particles are helpful in cooling applications.

**Keywords:** Carreau Fluid, Cattaneo-Christov heat flux model, Stretching sheet, Thermal radiation, Diffusion, Thermal and momentum slip boundary conditions

## **I. INTRODUCTION**

Many fluids of industrial significance, especially of the multi-phase nature (lubricants, emulsions, foams, slurries, dispersions and suspensions) and polymer melts and solutions (both natural and man-made), biological fluids (blood, saliva, synovial fluid) and liquids with special intermolecular forces (ionic liquids, magnetic liquids) exhibits complex flow behavior that diverge significantly from the classical Newtonian (Navier-Stokes) model. Accordingly, these fluids are classically known as non-Newtonian, non-linear or rheological complex fluids. Newtonian fluids have a constant viscosity and non-Newtonian fluids do not have constant viscosity, their viscosities strongly depend on the velocity gradients and they may display “elastic effects”. Various mathematical expressions have been suggested in the literature to model the flow diversity of non-Newtonian fluids. Such as Ostwald-De Waele model or power-law model, Sisko model, The Ellis model, The Carreau model, The Cross model, The Bingham model, The Herschel-Bulkey model, The Casson model, etc. Amongst these Fluid models four-parameter Carreau inelastic model [1] which was introduced in 1972 by Pierre Carreau caught the attention of many researchers and engineers [2-12]. Carreau fluid behaves as Newtonian at low shear rate and power law fluid at high shear rate. The Carreau fluid model is generally used to describe the time independent, shear-thinning category of non-Newtonian fluids. In particular Carreau model is used to

## International Journal of Innovative Research in Science, Engineering and Technology

(An ISO 3297: 2007 Certified Organization)

Vol. 6, Issue 11, November 2017

describe the flow characteristics of polymeric liquids like Xanthan and acacia gums, polyacrylamide gel solutions, biological fluid like blood [13-15]. Numerous investigators have focused on the theory of boundary layer flow, heat and mass transfer over a stretching sheet due to its various applications in manufacturing and chemical processes. In recent years several researchers have contributed towards boundary layer flow problem involving the stretching surfaces [16-19].

Over the decades, Fourier’s rule of heat conduction [20] has been considered the best model to predict the heat transfer behavior in various circumstances. The major drawback of Fourier’s rule of heat conduction is that produces a parabolic energy. And primary disturbance would affect the structure under attention. To overlook this paradox, in 1948 Cattaneo [21] modified the Fourier’s law for heat conduction by introducing relaxation time is well-defined as - time required to initiate steady state heat conduction after a temperature gradient is enforced. Whereas different materials have different thermal relaxation times, keeping this into view Christov [22] suggested a time derivative model and called it as Cattaneo–Christov heat flux model. Later on this model was used by many researchers to construct the energy equation and to analyze the heat transfer behavior of varied Newtonian and non-Newtonian fluids [23-26]. Afore mentioned studies invariably assumed “no-slip” condition at the boundary. However, no-slip situation is a hypothesis instead of a condition inferred from any principle and thus its authority has been debated constantly in the scientific literature. Slip properties have been revealed to be important in assured industrial thermal processing and manufacturing dynamical systems. Few recent attempts allowing for both the hydrodynamic and thermal slip impacts may be characterized by [27-30] and several studies therein.

The main motto of current investigation is to explore the steady boundary layer flow, heat and mass transfer mechanisms in MHD Carreau Dustyfluid past a stretched sheet with slip conditions. Of particular interest in the current work is to examine combined radioactive and Cattaneo-Christov heat flux model. Governing non-linear momentum, energy and concentration equations are transformed into dimensionless forms and are solved numerically by Runge-Kutta Fehlberg scheme.

### Formulation of the problem (Fig. 1)

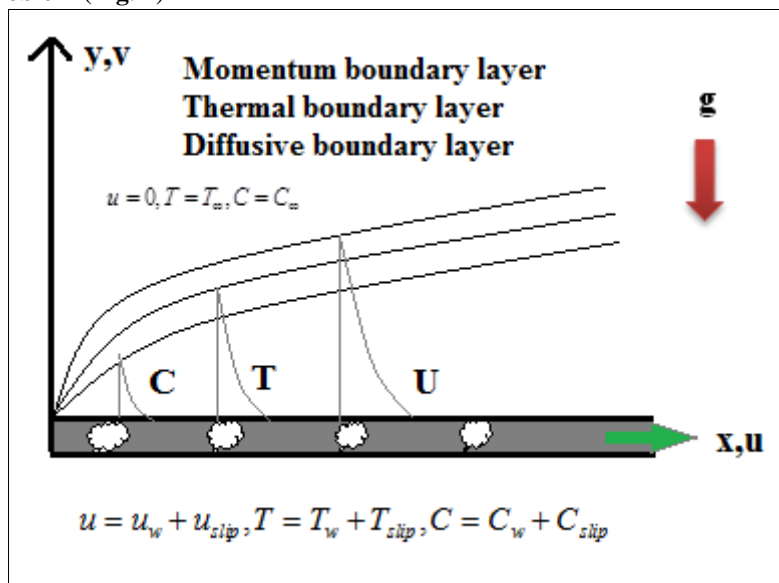


Fig. 1. Physical representation of the system.

## International Journal of Innovative Research in Science, Engineering and Technology

(An ISO 3297: 2007 Certified Organization)

Vol. 6, Issue 11, November 2017

Consider a steady slip flow of an incompressible, 2D, magneto hydrodynamic Carreau dusty fluid over a stretching sheet. The  $x$ -axis is taken as the direction of fluid motion and  $y$ -axis is vertical to the sheet. The flow is confined to the region  $y > 0$ . It is assumed that the sheet is stretched by two equal and opposite forces with the velocity  $u_w(x) = ax$ . Here  $a$  is positive constant. Along the  $y$ -axis a uniform magnetic field of strength  $B_0$  is imposed which generates magnetic effect in the  $x$ -direction. Dust particles are supposed to be spherical in shape and homogeneously distributed all the way through the fluid. It is assumed that the number density to be constant and volume fraction of dust particles can be neglected. The fluid and dust particle motion are coupled only through drag, heat and mass transfer between them. Stokes linear drag theory is used to model the drag force. The fluid temperature  $\theta(\xi)$  and concentration at the boundary and free stream are denoted by  $T_w, T_\infty$  and  $C_w, C_\infty$ . The magnetic Reynolds number is supposed to be small hence forth the induced magnetic field is neglected. Cattaneo-Christov heat flux and radiation heat flux are considered in this study. The constitutive equation for a Carreau fluid is given by [10];

$$\tau = \eta_\infty + (\eta_0 - \eta_\infty) \left[ 1 + \left( \Gamma \dot{\gamma} \right)^2 \right]^{\frac{n-1}{2}}$$

Where  $\eta_0$  is the zero-shear rate viscosity,  $\tau$  is the extra stress tensor,  $\eta_\infty$  is the infinite –shear rate viscosity,  $\Gamma$  is a material time constant and  $n$  is the power law index. The shear rate  $\dot{\gamma}$  is well-defined as

$$\dot{\gamma} = \sqrt{\frac{1}{2} \sum \sum \dot{\gamma}_{ij} \dot{\gamma}_{ji}} = \sqrt{\frac{1}{2} \Pi}$$

Where  $\Pi$  is the second invariant strain tensor. Based on the above expectations, the flow equations of continuity, momentum, energy and conservation of mass for both the fluid and dust phase takes the following for [19];

$$\frac{\partial u}{\partial x} + \frac{\partial v}{\partial y} = 0 \tag{1}$$

$$u \frac{\partial u}{\partial x} + v \frac{\partial u}{\partial y} = \frac{\mu}{\rho} \frac{\partial^2 u}{\partial y^2} \left[ 1 + \Gamma^2 \left( \frac{\partial u}{\partial y} \right)^2 \right]^{\frac{n-1}{2}} + \frac{\mu}{\rho} (n-1) \Gamma^2 \frac{\partial^2 u}{\partial y^2} \left( \frac{\partial u}{\partial y} \right)^2 \left[ 1 + \Gamma^2 \left( \frac{\partial u}{\partial y} \right)^2 \right]^{\frac{n-3}{2}} - \frac{\sigma B_0^2 u}{\rho} + \frac{KN}{\rho} (u_p - u) \tag{2}$$

$$\frac{\partial u_p}{\partial x} + \frac{\partial v_p}{\partial y} = 0 \tag{3}$$

$$u_p \frac{\partial u_p}{\partial x} + v_p \frac{\partial u_p}{\partial y} = \frac{K}{m} (u - u_p) \tag{4}$$

$$u \frac{\partial T}{\partial x} + v \frac{\partial T}{\partial y} + \lambda \left( u^2 \frac{\partial^2 T}{\partial x^2} + v^2 \frac{\partial^2 T}{\partial y^2} + \left( u \frac{\partial u}{\partial x} + v \frac{\partial u}{\partial y} \right) \frac{\partial T}{\partial x} + 2uv \frac{\partial^2 T}{\partial x \partial y} + \left( u \frac{\partial v}{\partial x} + v \frac{\partial v}{\partial y} \right) \frac{\partial T}{\partial y} \right) = \tag{5}$$

$$\frac{1}{\rho c_p} \left( K \frac{\partial^2 T}{\partial y^2} - \frac{\partial q_r}{\partial y} \right) + \frac{\rho_p c_p}{\tau_T} (T_p - T) + \frac{\rho_p}{\tau_v} (u_p - u)^2$$

$$u_p \frac{\partial T_p}{\partial x} + v_p \frac{\partial T_p}{\partial y} = - \frac{c_p}{c_m \tau_T} (T_p - T) \tag{6}$$

## International Journal of Innovative Research in Science, Engineering and Technology

(An ISO 3297: 2007 Certified Organization)

Vol. 6, Issue 11, November 2017

$$u \frac{\partial C}{\partial x} + v \frac{\partial C}{\partial y} = D_m \frac{\partial^2 C}{\partial y^2} + \frac{\rho_p}{\rho \tau_c} (C_p - C) \quad (7)$$

$$u_p \frac{\partial C_p}{\partial x} + v_p \frac{\partial C_p}{\partial y} = \frac{1}{\tau_c} (C - C_p) \quad (8)$$

Corresponding boundary conditions for the physical problem are given by

$$\text{at } y = 0: \quad u = K_1 \left( \frac{\partial u}{\partial y} \right) + u_w, \quad v = 0, \quad T = K_2 \left( \frac{\partial T}{\partial y} \right) + T_w, \quad C = K_3 \left( \frac{\partial C}{\partial y} \right) + C_w$$

$$\text{as } y \rightarrow \infty: \quad u \rightarrow 0, \quad u_p \rightarrow 0, \quad T \rightarrow T_\infty, \quad v_p \rightarrow v, \quad T_p \rightarrow T_\infty, \quad C \rightarrow C_\infty, \quad C_p \rightarrow C_\infty \quad (9)$$

Where  $(u, u_p)$  and  $(v, v_p)$  are the velocity mechanisms along the  $x$  and  $y$  direction of the fluid and dust particle phase,  $\rho$  and  $\rho_p = mN$  are the density of the dust and fluid particle phase,  $m$  and  $N$  are the mass and number density of the dust particles per unit volume,  $\mu$  is the dynamic viscosity of the fluid,  $\sigma$  is the electrical conductivity,  $B_0$  is the uniform magnetic field,  $k = 6\pi\mu r$  is the stokes resistance (drag coefficient) and  $r$  is the radius of the dust phase.  $T$  and  $T_p$  are the temperature of the fluid and dust particle,  $c_p$  and  $c_m$  are the specific heat of fluid and dust particles,  $\tau_T$  represents the thermal equilibrium time.  $\tau_v$  represents the dust phase relaxation time  $k$  is the thermal conductivity of the fluid and  $q_r$  is the radioactive heat flux.  $\sigma^*$  is the Stefan – Boltzmann constant and  $K^*$  is the mean absorption coefficient.  $C$  and  $C_p$  are the concentration species of the fluid and dust particle phase; the dust particles gain mass concentration from the fluid by diffusion through their spherical surface.  $D_m$  is the Brownian mass diffusivity coefficient,  $\tau_c$  is the time required by dust particles to adjust its concentration relative to the fluid.  $K_1$ ,  $K_2$  and  $K_3$  are the hydrodynamic, thermal, and concentration slip factors.

The Roseland diffusion flux model is used for the thermal radiation heat transfer and is given by

$$q_r = -\frac{4\sigma^*}{3K^*} \frac{\partial T^4}{\partial y}$$

From Taylor's series

$$T^4 \cong 4T_\infty^3 T - 3T_\infty^4$$

Substituting this expression into equation (5) energy equation leads to the following form:

$$u \frac{\partial T}{\partial x} + v \frac{\partial T}{\partial y} + \lambda \left( u^2 \frac{\partial^2 T}{\partial x^2} + v^2 \frac{\partial^2 T}{\partial y^2} + \left( u \frac{\partial u}{\partial x} + v \frac{\partial u}{\partial y} \right) \frac{\partial T}{\partial x} + 2uv \frac{\partial^2 T}{\partial x \partial y} + \left( u \frac{\partial v}{\partial x} + v \frac{\partial v}{\partial y} \right) \frac{\partial T}{\partial y} \right) = \frac{1}{\rho c_p} \left( K + \frac{16\sigma^* T_\infty^3}{3K^*} \right) \frac{\partial^2 T}{\partial y^2} + \frac{\rho_p c_p}{\tau_T} (T_p - T) + \frac{\rho_p}{\tau_v} (u_p - u)^2 \quad (10)$$

To transform the governing equations into a set of ordinary equations, we bring together the succeeding transformation as,

$$u = axf'(\zeta), \quad \zeta = \left( \frac{a}{v} \right)^{0.5} y, \quad v = -\sqrt{va} f(\zeta)$$

$$u_p = axF'(\zeta), \quad v_p = -\sqrt{va} F(\zeta),$$

$$T = (T_w - T_\infty)\theta(\zeta) + T_\infty, \quad T_p = (T_w - T_\infty)\theta_p(\zeta) + T_\infty$$

$$C = (C_w - C_\infty)\phi(\zeta) + C_\infty, \quad C_p = (C_w - C_\infty)\phi_p(\zeta) + C_\infty \quad (11)$$

## International Journal of Innovative Research in Science, Engineering and Technology

(An ISO 3297: 2007 Certified Organization)

Vol. 6, Issue 11, November 2017

Where a prime denote differentiation with respect to  $\xi$ . Continuity equations (1) and (3) are identically satisfied. Equations (2), (4)-(9) are transformed as follows.

$$f'''(\xi) \left[ 1 + \left( \frac{n-1}{2} \right) We f''(\xi)^2 \left( 3 + (n-3) We f''(\xi)^2 \right) \right] - \left( f'(\xi)^2 \right) + f(\xi) f''(\xi) \quad (12)$$

$$+ l \beta_v \left[ F'(\xi) - f'(\xi) \right] - M f'(\xi) = 0$$

$$F''(\xi) F(\xi) - \left( F'(\xi)^2 \right) + \beta_v \left[ f'(\xi) - F'(\xi) \right] = 0 \quad (13)$$

$$\left( \frac{1}{Pr} \right) (1 + Nr) \theta''(\xi) + l \beta_T (\theta_p(\xi) - \theta(\xi)) + l \beta_v Ec (F'(\xi) - f'(\xi))^2 \quad (14)$$

$$+ f(\xi) \theta'(\xi) - \Lambda \left( f(\xi)^2 \theta''(\xi) + f(\xi) f'(\xi) \theta'(\xi) \right) = 0$$

$$\theta_p'(\xi) F(\xi) - \gamma \beta_T (\theta_p(\xi) - \theta(\xi)) = 0 \quad (15)$$

$$\phi''(\xi) + Sc f(\xi) \phi'(\xi) + Sc l \beta_c (\phi_p(\xi) - \phi(\xi)) = 0 \quad (16)$$

$$\phi_p'(\xi) F(\xi) + \beta_c (\phi(\xi) - \phi_p(\xi)) = 0 \quad (17)$$

The transformed boundary conditions are

$$f'(0) = 1 + \alpha_1 f''(0), \quad f(0) = 0, \quad \theta(0) = 1 + \alpha_2 \theta'(0), \quad \phi(0) = 1 + \alpha_3 \phi'(0) \quad (18)$$

$$f'(\infty) = 0, \quad F'(\infty) = 0, \quad F(\infty) \rightarrow f(\infty), \quad \theta(\infty) = 0, \quad \theta_p(\infty) = 0, \quad \phi(\infty) = 0, \quad \phi_p(\infty) = 0$$

Where  $\alpha_1 = K_1 \sqrt{\frac{a}{\nu}}$  is the velocity slip,  $\alpha_2 = K_2 \sqrt{\frac{a}{\nu}}$  is the thermal slip,  $\alpha_3 = K_3 \sqrt{\frac{a}{\nu}}$  is the concentration slip.

$M = \frac{\sigma B_0^2}{\rho b}$  is the magnetic field.  $l = \frac{Nm}{\rho}$  is the mass concentration parameter of dust particles.  $\tau_v = \frac{m}{K}$  is the dust

phase relaxation time.  $We = \frac{a u_w^2 \Gamma^2}{\nu}$  is the Weissenberg number.  $\beta_v = \left( \frac{1}{b \tau_v} \right)$  is the fluid -particle interaction

parameter,  $Pr = \frac{\mu c_p}{K}$  is the Prandtl number,  $Ec = \frac{u_w^2}{c_p (T_w - T_\infty)}$  is the Eckert number,  $\Lambda = \lambda a$  is the thermal

relaxation time,  $Nr = \frac{16 \sigma^* T_\infty^3}{3 K K^*}$  is thermal Radiation,  $\gamma = \frac{c_p}{c_m}$  is the specific heat ratio,  $Sc = \frac{\nu}{D_m}$  is the Schmidt

number,  $\beta_c = \frac{1}{b \tau_c}$  is concentration fluid particle interaction,  $\beta_T = \frac{1}{b \tau_t}$  is the temperature fluid particle interaction.

Distinctive measures of practical attention are skin friction coefficient  $C_f$ , local Nusselt  $Nu_x$  and local Sherwood number  $Sh_x$ , Which are defined as ;

$$Nu_x = \frac{x q_w}{k (T_\infty - T_w)}, \quad C_f = \frac{\tau_w}{\rho U_w^2}, \quad \text{and} \quad Sh = \frac{x j_w}{D_m (C_w - C_\infty)} \quad (19)$$

# International Journal of Innovative Research in Science, Engineering and Technology

(An ISO 3297: 2007 Certified Organization)

Vol. 6, Issue 11, November 2017

Where the surface shear stress ( $\tau_w$ ), surface heat flux ( $q_w$ ) and surface mass flux ( $j_w$ ) are given by;

$$\tau_w = \mu_0 \left( \frac{\partial u}{\partial y} + \left( \frac{n-1}{2} \right) \Gamma^2 \left( \frac{\partial u}{\partial y} \right)^3 \right)_{y=0}, \quad q_w = -k \left( \frac{\partial T}{\partial y} \right)_{y=0}, \quad j_w = -D_m \left( \frac{\partial c}{\partial y} \right)_{y=0} \quad (20)$$

Using the non-dimensional variables, we obtain

$$\sqrt{\text{Re}_x} C_f = \left[ f''(\zeta) + \frac{(n-1)We^2}{2} (f'''(\zeta))^3 \right]_{\zeta=0}, \quad Nu_x = -\text{Re}_x^{\frac{1}{2}} \theta'(0), \quad Sh = -\text{Re}_x^{\frac{1}{2}} \phi'(0)$$

Where  $\text{Re}_x = \left( \frac{xu_w(x)}{\nu} \right)$  the local Reynolds number.

## II. NUMERICAL RESULTS AND DISCUSSION

The set of nonlinear ODEs (12)-(17) with the BC (18) are solved numerically by employing shooting technique coupled together 45 order RKF method by considering pertinent parameters  $We=0.2, Nr=0.5, Sc=2, M=0.5, \alpha_1=0.1, \alpha_2=0.1, \alpha_3=0.1, \lambda=0.2, l=0.3, \beta_c=0.3, \beta_v=0.3, \beta_f=0.3, n=0.5, Pr=4, Ec=0.2, \gamma=0.2$ . These values are taken constant during the entire analysis procedure, except the variations in the considered figures and tables. Table 1 display the validation of local Nusselt number for varied values of Pr. The present results are compared with available results in the literature. Ishak et al. [25], El-Aziz [17] and Krupa Lakshmi et al. [19] and found excellent agreement for all the values of parameters considered. In figures solid line indicates the fluid phase profiles and dashed lines refers the dust phase profiles of the flow.

Pr	Present Studies	Krupa Lakshmi [19]	Ishak [25]	El-Aziz [17]
0.72	0.80859	0.80863	0.8086	0.80873
1	1	1	1	1
23	1.92357	1.92367	1.9237	1.92368
10	3.72068	3.72067	3.7207	3.7207
100	12.2942	12.294087	12.2941	12.2941

**Table 1.** Validation of the  $-\theta'(0)$  for the case of  $n=1, R=l=We=\lambda=Ec=\alpha_1=M=0, \alpha_1=\alpha_2=\gamma=0$ .

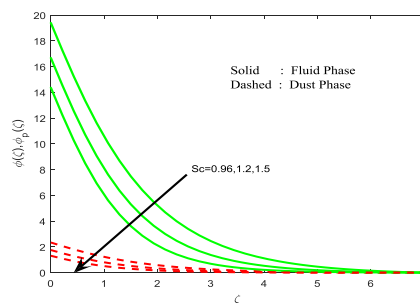


**Fig. 2.** Concentration profiles for various values of Schmidt number-Sc.

# International Journal of Innovative Research in Science, Engineering and Technology

(An ISO 3297: 2007 Certified Organization)

Vol. 6, Issue 11, November 2017

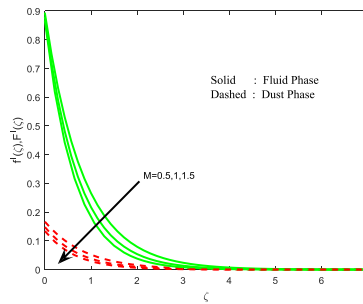


Fig. 3. Velocity distributions for various values of magnetic field  $M$ .

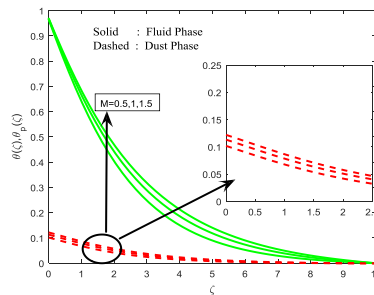


Fig. 4. Temperature distributions for various values of magnetic field  $M$ .

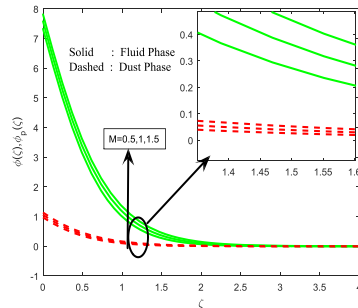


Fig. 5. Concentration profiles for different values of magnetic field  $M$ .

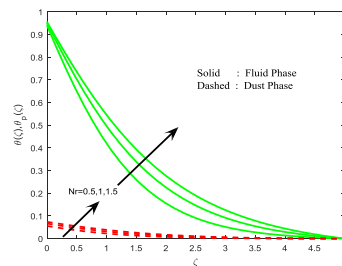


Fig. 6. Temperature profiles for different values of thermal radiation  $Nr$ .

# International Journal of Innovative Research in Science, Engineering and Technology

(An ISO 3297: 2007 Certified Organization)

Vol. 6, Issue 11, November 2017

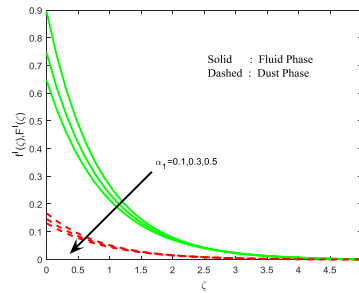


Fig. 7. Velocity profiles for various values of velocity slip.

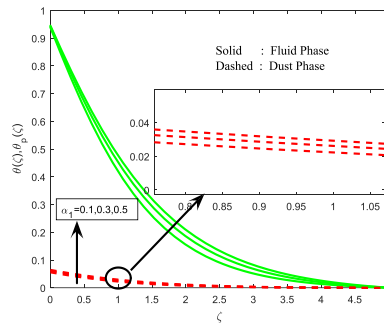


Fig. 8. Temperature profiles for various values of velocity slip.

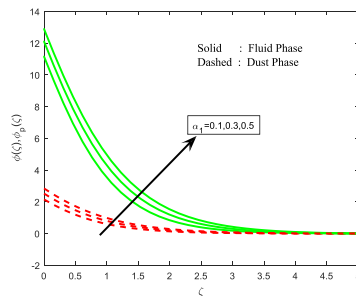


Fig. 9. Concentration profile for different values of velocity slip.

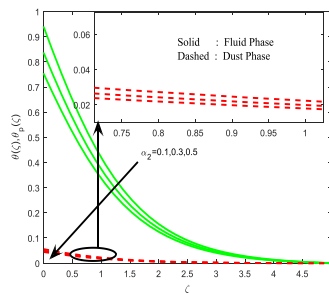


Fig. 10. Temperature profiles for different values of thermal slip.

# International Journal of Innovative Research in Science, Engineering and Technology

(An ISO 3297: 2007 Certified Organization)

Vol. 6, Issue 11, November 2017

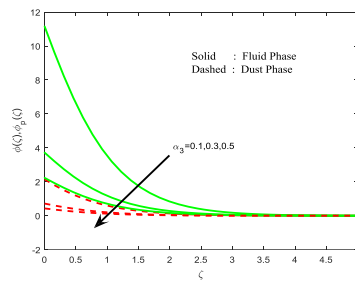


Fig. 11. Concentration fields for different values of concentration slip.

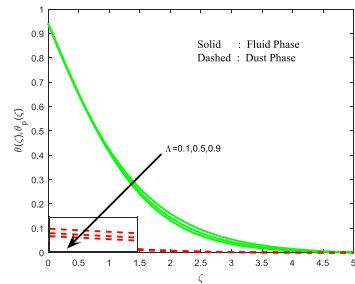


Fig. 12. Temperature fields for different values of thermal relaxation time.

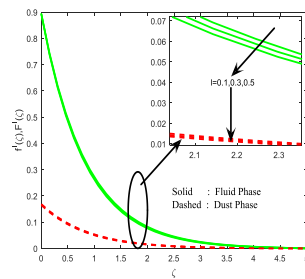


Fig. 13. Velocity profiles for various values of dust particles mass concentration parameter.

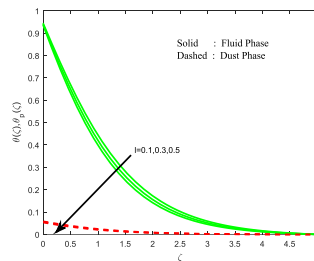


Fig. 14. Temperature profiles for various values of dust particles mass concentration parameter.

# International Journal of Innovative Research in Science, Engineering and Technology

(An ISO 3297: 2007 Certified Organization)

Vol. 6, Issue 11, November 2017

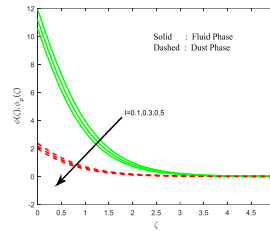


Fig. 15. Concentration profiles for various values of dust particles mass concentration parameter.

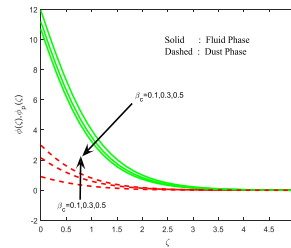


Fig. 16. Concentration profiles for different values of fluid particle interaction.

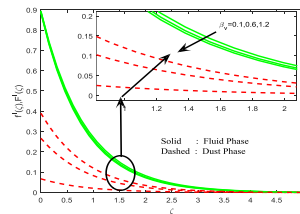


Fig. 17. Velocity fields for different values of fluid particle interaction.

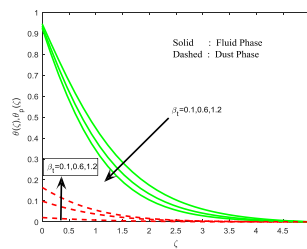


Fig. 18. Temperature field for different values of fluid particle interaction.

Fig. 2 displays the effect of  $Sc$  on concentration field of dust and fluid phase. It is interesting to note that trends of both fluid and dust phase decrease with the accelerating values of ( $Sc$ ). Hence, one may anticipate that expansion in ( $Sc$ ) shows noteworthy reduction in the molecular diffusion which results, decrease in thickness of the solutal boundary layer. Figs. 3-5 illustrate the effect of magnetic field on the velocity  $f'(\xi)$ , temperature  $\theta(\xi)$  and concentration profiles for both dust and fluid phases. It is noticeable from the figures that enhancement in magnetic field parameter declines the velocity profiles  $f'(\xi)$  but enhances the temperature  $\theta(\xi)$  and concentration  $\phi(\xi)$  profiles for both dust and fluid phases.

From Fig. 6 the nature of temperature distributions with reference to variable values of thermal radiation parameter ( $N_r$ ) can be visualized. An Increment in the radiation parameter ( $N_r$ ) leads to higher temperature profiles across the boundary region, resulting in the thermal boundary layer thickness for both fluid and dust phases. Hence the radiation

## International Journal of Innovative Research in Science, Engineering and Technology

(An ISO 3297: 2007 Certified Organization)

Vol. 6, Issue 11, November 2017

effect must be at its minimum in industrial applications in order to enable cooling process. Figs. 7-9 indicates that slip coefficient has significant impact on the velocity, temperature and concentration profiles. With an increase in the velocity slip parameter  $\alpha_1$  fluid phase and dust phase velocity amplitude decreases because flow experience less drag and propulsion of the stretching sheet is moderately transmitted to the fluid. One can also observe smooth decaying in the velocity profiles hence good convergence in the numerical solution is seen. From Figs. 8 and 9 it is clear that rise in velocity slip parameter  $\alpha_1$  temperature and concentration profiles increases.

M	Nr	$\alpha_1$	$\alpha_2$	$\alpha_3$	$\wedge$	$l$	$\beta_c$	$\beta_v$	$-CfRe_x^{1/2}$	$NuRe_x^{1/2}$	$ShRe_x^{-1/2}$
0.9									1.079651	0.600437	10
1.2									1.225868	0.564593	10
1.5									1.351195	0.539367	10
	0.5								1.079795	1.032121	10
	1								1.079795	1.212521	10
	1.5								1.079795	1.377559	10
		0.1							1.079795	1.032121	10
		0.3							0.853581	0.964833	10
		0.5							0.710927	0.917086	10
			0.1						1.079795	1.032121	10
			0.3						1.079795	0.91778	10
			0.5						1.079795	0.826247	10
				0.1					1.079795	1.032121	10
				0.3					1.079795	1.032121	3.333333
				0.5					1.079795	1.032121	2
					0.1				1.079795	1.032757	10
					0.5				1.079795	1.026551	10
					0.9				1.079795	1.01153	10
						0.1			1.064171	0.956949	10
						0.3			1.079795	1.032121	10
						0.5			1.095206	1.101267	10
							0.1		1.065302	1.039924	10
							0.6		1.09602	1.024615	10
							1.2		1.118065	1.01627	10
								0.1	1.079795	0.948918	10
								0.6	1.079795	1.13507	10
								1.2	1.079795	1.293011	10

**Table 2.** Shows the impact of non-dimensional parameters on skin friction coefficient, local Sherwood and Nusselt numbers.

In Fig. 10 one can observe a rise in thermal slip parameter  $\alpha_2$  temperature of the fluid phase and dust phase falls rapidly. Heat transfer from the stretching sheet to the fluid becomes slower. When compared to the free stream maximum effect is observed at the surface temperature. Since the amount of heat transferred from the stretching sheet to the flow is decreased there is decline in temperature. But flow temperature converges smoothly. From Fig. 11 it is evident that the enhancement in the concentration slips parameter decreases the concentration profile of both fluid and dust phase. The influence of thermal relaxation parameter on thermal boundary layers is observed in Fig. 12 it is noticeable that accelerating values of thermal relaxation time correspond to a fall in the thermal boundary layer in case of both fluid and dust phase. Physically increasing value of the thermal relaxation facilitates the gap among the fluid molecule hence material particles require extra time in order to allocation heat to its adjacent particles which results in temperature decline. Figs. 13-15 exhibits the influence of dust particle mass concentration towards dust and fluid phase velocity, temperature and concentration profiles. An internal friction is experienced within the fluid by the introduction of dust particles in the flow hence there is a net retardation in the flow. Figs. 16-18 displays the influence of  $\beta_c, \beta_v, \beta_t$  on concentration, velocity ( $f'(\xi), F(\xi)$ ) and temperature profiles of fluid and dust phase. It is interesting to note that

## International Journal of Innovative Research in Science, Engineering and Technology

(An ISO 3297: 2007 Certified Organization)

Vol. 6, Issue 11, November 2017

accelerating values of  $\beta_c, \beta_v, \beta_t$  declines respective concentration, velocity ( $f'(\xi), F(\xi)$ ) and temperature profiles of fluid phase where as significant increase in profiles are seen in dust phase (Table 2).

It is evident that the rise in magnetic field parameter reduces skin friction coefficient along with heat transfer rate but the mass transfer rate remains constant. Skin friction coefficient and mass transfer rate remains constant whereas heat transfer rate increases with the increase in the thermal radiation parameter ( $Nr$ ). Rise in mass concentration of dust particles (1) depreciates friction coefficient improves heat transfer rate  $NuRe_x^{1/2}$  and mass transfer rate  $ShRe_x^{-1/2}$  remains constant. It is apparent that the increase in thermal relaxation time heat transfer rate  $NuRe_x^{1/2}$  decreases whereas the mass transfer rate  $ShRe_x^{-1/2}$  and friction coefficient  $-CfRe_x^{1/2}$  remains unaltered. Velocity slip raises friction coefficient decreases heat transfer rate, but shows no effect on mass transfer rates. Rise in Thermal slip decrease the heat transfer rate, but no change is observed in friction coefficient and mass transfer rate. Increase in diffusion slip parameter lessons the mass transfer rate, but no effect on friction coefficient and the heat transfer rate.

### III. SUMMARY

In the present study mathematical model has been considered for the flow, heat and mass transfer of Carreau Dusty fluid past a stretching sheet with the slip condition at the boundary. The impact of several dimensionless parameters on the velocity, temperature and concentration profiles together with a local Nusselt number, Skin friction coefficient and Sherwood number are distributed through tables and plots. The main outcomes of this study are as follows:

- The rate of mass transfer decreases with the rise in Schmidt number.
- Magnetic field parameter inhibits the velocity profiles, but boosts the heat transfer and mass transfer rate.
- As the thermal radiation parameter increases the rate of heat transfer increase.
- Increase in the velocity slip factor reduces the velocity boundary layer thickness, but improves the temperature and concentration profiles.
- A rise in thermal slip parameter reduces the temperature and the rate of heat transfer.
- Increase in the concentration slip parameter reduces the species concentration.
- Temperature as well as thermal boundary layer thickness is decreasing functions of thermal relaxation time.
- An increase in the dust particle mass concentration parameter reduces the velocity, thermal boundary and concentration boundary layer thickness.

Increase in fluid particle interaction parameter  $\beta_v, \beta_t$  and  $\beta_c$  velocity, temperature and concentration profiles of fluid phase decreases but reverse trend are observe dindust phase.

### REFERENCES

- [1] P.J. Carreau, "Rheological equations from molecular network theories", Trans. Soc. Rheol, vol. 116 pp.99-127, 1972.
- [2] A.M. Sobh, "Slip flow in a peristaltic transport of a Carreau fluid in an asymmetric channel", Can. J. Phys, vol.87 pp.1-9, 2009.
- [3] N. Ali, T. Hayat, "Peristaltic motion of a Carreau fluid in an asymmetric channel", Appl. Math. Comput, vol.193, pp.535-552, 2007.
- [4] T. Hayat, N. Saleem, N. Ali, "Effect of induced magnetic field on peristaltic transport of a Carreau fluid", Commun Nonlinear Sci Numer Simulat, vol.15, pp.2407-2423, 2010.
- [5] N.S. Akbar, S. Nadeem, R.H. ShiweiYe, "Stagnation point flow of Carreau fluid toward a permeable shrinking sheet: Dual solutions", A in Shams Engineering Journal. 2014.
- [6] T. Hayat, S. Asad, M. Mustafa, A. Alsaedi, "Boundary layer flow of Carreau fluid over a Convectively heated stretching sheet", Applied Mathematics and Computation, vol.246, pp.12-22, 2014.
- [7] C.S.K. Raju, S.M. Ibrahim, S. Anuradha, P. Priyadharshini, "Bio-Convection on the nonlinear radioactive flow of a carreau fluid over a moving wedge with suction or injunction", The European Physical Journal plus vol. 131 no.11, pp.409, 2016.
- [8] M. Khan, Hashim, "Boundary layer flow and heat transfer to Carreau fluid over a non-linear stretching sheet, AIP Advances ,5(2015)1-14.
- [9] B.J. Olajuwon, Convective heat and mass transfer in a hydromagnetic Carreau fluid past a vertical porous plated in presence of thermal radiation and thermal diffusion", Therm. Sci, vol.15, pp.241-252, 2011.
- [10] C.S.K. Raju, N. Sandeep, "Falkner-Skan flow of a magnetic-Carreau fluid past a wedge in the presence of cross diffusion effects", The European Physical Journal Plus. 2016.

# International Journal of Innovative Research in Science, Engineering and Technology

(An ISO 3297: 2007 Certified Organization)

Vol. 6, Issue 11, November 2017

- [11] CSK. Raju, N. Sandeep, "Heat and mass transfer in MHD non-Newtonian bio-convection flow over a rotating cone/plate with cross diffusion", Journal of molecular liquids, vol.215, pp.115-126, 2016.
- [12] M. Khan, M. Azam, "Unsteady heat and mass transfer mechanisms in MHD Carreaunanofluid flow", Journal of Molecular Liquids, vol.225, pp.554-562, 2017.
- [13] M. Lukacova-Medvid'ova, A. Zauskova, "Numerical modelling of shear-thinning non-Newtonian flows in compliant vessels", International Journal for Numerical Methods in fluids, vol. 56 no.8, pp.1409-1415, 2008.
- [14] S. Desplanques, F. Renou, M.Grisel, C. Malhiac, "Impact of chemical composition of xanthan and acacia gums on the emulsification and stability of oil-in-water emulsion", Food Hydrocolloids, vol. 27 no.2, pp. 401-410, 2012.
- [15] BC. Sakiadis, "Boundary Layer Behavior on Continuous Solid Surfaces: II Boundary Layer on a Continuous Flat Surface", AIChE Journal, Vol.7 no.2, pp.221-225, 1961.
- [16] LJ. Crane, "Flow past a stretching sheet", Zeit. Angew. Math. Phys, vol. 21 pp. 645-647, 1970.
- [17] MA. Aziz, "Mixed convection flow of a micropolar fluid from an unsteady stretching surface with viscous dissipation", Journal of the Egyptian Mathematical Society vol. 21 pp.385-394, 2013.
- [18] CSK. Raju, N. Sandeep, C. Sulochana, V. Sugunamma, M. JayachandraBabu, "Rasdiation, inclined magnetic field and cross-diffusion effects on flow over a stretching surface", Journal of the Nigerian Mathematical Society, vol. 34 no.2, pp.169-180, 2015.
- [19] KLK. Lakshmi, BJ. Gireesha, RSR. Gorla, B. Mahantesh, "Two-phase Boundary Layer Flow, Heat and Mass Transfer of a Dusty Liquid past a Stretching Sheet with Thermal Radiation", Int J Industrial Mathematics, Vol. 8, No.3, pp.14, 2016.
- [20] JBJ. Fourier, "Theorieanalytique de la chaleur Paris, 1822.
- [21] C. Cattano, S. Conduzionedelcalore, "AttitudelSeminarioMaermaticoeFisico" dell Universita di Modena e Reggio Emilia, vol.3 pp.481-486, 1948.
- [22] Cl. Christov, "On frame indifferent formulation of the Maxwell-Cattaneo model of finite - speed heat conduction", Mech Res Commun, vol.36 pp.481-486, 2009.
- [23] ME. Ali, N. Sandeep, "Cattaneo-Christov model for irradiative heat transfer of magnetohydrodynamic Casson-ferrofluid: A numerical study", Results in Physics, vol.7 pp. 21-30, 2017.
- [24] M. Mustafa, Cattaneo-Christov "Heat flux model for rotating flow and heat transfer of upper-convicted Maxwell fluid", AIPAdv, vol.5 047109, 2015.
- [25] A. Ishak, R. Nazar, I. Pop, "Boundary layer flow and heat transfer over an unsteady stretching vertical surface", Meccanica, vol.44 pp.369-375, 2009.
- [26] MM. Bhatti, A. Zeeshan, N. Ijaz, O. Anwar Beg, A. Kadir, "Mathematical modeling of nonlinear thermal radiation effects on EMHD peristaltic pumping of viscoelastic dusty fluid through a porous medium duct", Engineering Science and Technology, an International Journal.
- [27] EM. Sparrow, SH. Lin, "Laminar heat transfer in tubes under slip-flow conditions", ASME J. Heat Transfer, vol. 84, pp.363-639, 1962.
- [28] A. SubbaRao, V. Ramachandra Prasad, K. Harshavalli, O. Anwar Beg, "Thermal Radiation Effects On Non-Newtonian Fluid In A Variable Porosity Regime With Partial Slip", Journal of Porous Media, vol. 19 no.4, pp.1-17, 2016.
- [29] HI. Andersson, Trondheim, Norway, "Slip flow past a stretching surface", Acta Mechanica, vol.158, pp.121-125, 2002.
- [30] A. Aziz, "Hydrodynamic and thermal slip flow boundary layers over a flat plate with constant heat flux boundary condition", Commun Nonlinear Sci Numer Simulat, vol. 15, pp.573-580, 2010.